(24) (a) R. R. Ernst, *Adv. Magn. Reson.*, **2**, 1 (1966); (b) G. A. Petersson, Ph.D. Thesis, California Institute of Technology, 1970; (c) W. M. Wittbold, Jr., private communication.
(25) "NTCFT, Version 1002", Nicolet Technology Corp., Mountain View, Calif., 1975.
(26) (a) A. A. Bothner-By and S. M. Castellano in "Computer Programs for Chemistry", Vol. 1, D. F. DeTar, Ed., W. A. Benjamin, New York, 1968, pp 10–53; (b) "Itrcal", Nicolet Instrument Corp., Madison, Wis., 1973.
(27) See data for free amino acids in D_2O reported in Table I of G. C. K. Roberts and O. Jardetzky, *Adv. Protein Chem.*, **24**, 447 (1970), and previous work of others quoted therein.
(28) Sodium 2,2-dimethyl-2-silapentane-5-sulfonate was used as the internal standard for the chemical shifts reported in ref 27, but the difference between this standard and TSP, which we use in the work that we report here, is negligible for our purposes.
(29) W. Saur, H. L. Crespi, and J. J. Katz, *J. Magn. Reson.*, **2**, 47 (1970), and references cited therein.
(30) F. A. Bovey, "Nuclear Magnetic Resonance Spectroscopy", Academic Press, New York, 1969, pp 105–113.
(31) A. I. R. Brewster and V. J. Hruby, *Proc. Natl. Acad. Sci.U.S.A.*, **70**, 3806 (1973).
(32) A. J. Fischman, Ph.D. Thesis, The Rockefeller University, 1978.
(33) I. Fric, M. Kodicek, M. Flegel, and M. Zaoral, *Eur. J. Biochem.*, **56**, 493 (1975).
(34) R. Walter, H. R. Wyssbrod, and J. D. Glickson, *J. Am. Chem. Soc.*, **99**, 7326 (1977).
(35) R. Walter, *Fed. Proc., Fed. Am. Soc. Exp. Biol.*, **36**, 1872 (1977).
(36) R. Walter, C. W. Smith, P. K. Mehta, S. Boonjarern, J. A. L. Arruda, and N. A. Kurtzman in "Disturbances in Body Fluid Osmolality", T. E. Andreoli, J. J. Grantham, and F. C. Rector, Jr., Eds., American Physiological Society, Bethesda, Md., 1977, pp 1–36.
(37) See ref 16 for the method of calculating these populations and for definitions of rotameric states I–III; assignments of populations to states I and II are equivocal—i.e., assignments may be interchanged—unless the stereochemical assignments of the *pro-R* and *pro-S* C^{β} protons can be unequivocally made (e.g., see A. J. Fischman, H. R. Wyssbrod, W. C. Agosta, and D. Cowburn, *J. Am. Chem. Soc.*, **100**, 54 (1978), for a discussion of this problem).
(38) Feeney et al. (ref 10b) state that the observed shifts of the C^{δ} and C^{ϵ} protons of Tyr^2 of LVP in aqueous solution can result from a stacking interaction in which the two aromatic rings of Tyr^2 and Phe^3 spend approximately one-third of their time in a conformation where the two rings are coplanar and partially overlapping, but they do not give the conformational parameters used in their calculation; they also mention that similar shifts are observed in the simple dipeptide Tyr-Phe.
(39) Walter et al. (ref 36) discuss several possibilities for different orientations of the side chain of Gln^4 in the various neurohypophyseal hormones.
(40) See Table II of ref 27.

Molecular Structures of the Dihydrodiols and Diol Epoxides of Carcinogenic Polycyclic Aromatic Hydrocarbons. X-ray Crystallographic and NMR Analysis

D. E. Zacharias,[1a] J. P. Glusker,*[1a] P. P. Fu,[1b] and R. G. Harvey[1b]

Contribution from The Institute for Cancer Research, The Fox Chase Cancer Center, Philadelphia, Pennsylvania 19111, and The Ben May Laboratory for Cancer Research, The University of Chicago, Chicago, Illinois 60637. *Received November 13, 1978*

Abstract: The molecular dimensions and conformations of the *trans*-1,2- and 10,11-dihydrodiols of benz[*a*]anthracene have been determined from X-ray crystal structure analyses. The cell dimensions are $a = 14.399$ (3) Å, $b = 7.942$ (2) Å, $c = 11.579$ (3) Å, $\beta = 100.93$ (2)°, space group $P2_1/c$ for the 1,2-dihydrodiol, and $a = b = 18.905$ (3), $c = 7.529$ (1) Å, space group $P4_2/n$ for the 10,11-dihydrodiol. The trans hydroxyl groups are axial in the 1,2-dihydrodiol; the bulk of H(12) would be presumed to hinder the formation of the diequatorial conformer of the diol. This steric problem does not exist for the 10,11-dihydrodiol and the hydroxyl groups in the molecule in the crystalline state are diequatorial. NMR analyses in solutions of deuterated chloroform, acetone, or dimethyl sulfoxide give results which indicate that the diaxial conformation also predominates for the 1,2-dihydrodiol in solution. In the case of the less hindered 10,11-dihydrodiol there is an equilibrium of approximately 30% diaxial and 70% diequatorial conformers in solution. The experimentally determined dimensions for these two trans diols, together with previously determined dimensions of arene oxides, have given sufficient data for the calculation of approximate dimensions for the diol epoxides of benz[*a*]anthracene and of benzo[*a*]pyrene which have been implicated as the ultimate carcinogenic metabolites of these hydrocarbons. A characteristic of the covalent bond formed to a biological macromolecule from an atom in the bay region of an activated polycyclic aromatic hydrocarbon is that it is *axial* as a result of steric hindrance.

Introduction

Trans dihydrodiols are among the principal metabolites of carcinogenic polycyclic arenes in mammalian cells.[2] While the majority undergo detoxification via conjugation and excretion, a significant proportion are metabolically transformed by the microsomal enzymes to diol epoxide derivatives. Many of the latter are highly mutagenic,[3-9] and the "bay region"[10] anti isomeric diol epoxides have been implicated as the principal ultimate active forms of benzo[*a*]pyrene[11] and other carcinogenic hydrocarbons.[6,7,12-15]

The factors which determine whether a particular dihydrodiol will undergo detoxification or activation are at present poorly understood. Since these pathways are likely to be dependent upon the molecular structures of the compounds involved, we have undertaken to investigate the structures of selected dihydrodiol metabolites by X-ray crystallographic analysis. We reported previously[16] the structure of (±)-*cis*-5,6-dihydro-5,6-dihydroxy-7,12-dimethylbenz[*a*]anthracene, a representative "K-region"[10] dihydrodiol. We report here the crystal structures of (±)-*trans*-1,2-dihydro-1,2-dihydroxybenz[*a*]anthracene (**1**) and (±)-*trans*-10,11-dihydro-10,11-dihydroxybenz[*a*]anthracene (**2**), representative

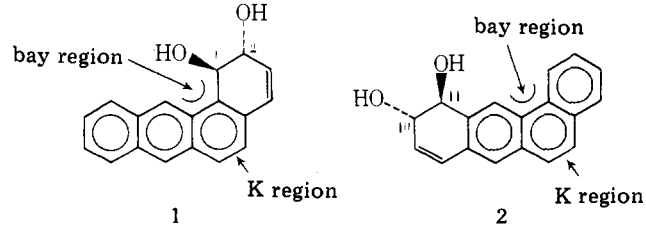

non-K-region dihydrodiols in bay region and non-bay-region benzo rings, respectively. Although satisfactory crystals of the diol epoxides themselves could not be obtained, the analysis described herein provides three-dimensional coordinates from which it has proven possible to derive coordinates for the cor-

0002-7863/79/1501-4043$01.00/0

Table I

A. Crystal Data

	1	2
molecular formula	$C_{18}H_{14}O_2$	$C_{18}H_{14}O_2$
formula weight	262.31	262.31
crystal system	monoclinic	tetragonal
systematic absences	$h0l$, l odd; $0k0$, k odd; $00l$, l odd	$hk0$, $h + k$ odd; $00l$, l odd
space group	$P2_1/c$	$P4_2/n$
cell dimensions	a = 14.399 (3) Å b = 7.942 (2) Å c = 11.579 (3) Å β = 100.93 (2)° V = 1300.2 (6) Å^3	a = 18.905 (3) Å b = 18.905 (3) Å c = 7.529 (1) Å V = 2602.1 (6) Å^3
calcd density	1.34 g cm^{-3}	1.34 g cm^{-3}
molecules per cell	4	8
$F(000)$	1104	2208
crystal shape and size	isosceles triangle base = 0.7, altitude = 0.45, × 0.1 mm	prism 0.3 × 0.3 × 0.6 mm

B. Experimental

	1	2
no. of data collected	2549	2584
no. of data above threshold	2298 ($1.5\sigma(I)$)	2338 ($2.0\sigma(I)$)
δ	0.016	0.020

C. Refinement Results

	1	2
final residual (R) (obsd data)	0.069	0.059
final weighted residual (wR) (obsd data)	0.104	0.087
weighting function	$F < 0.4$, $\sigma(F) = 0.0$ $0.4 \leq F \leq 3.0$, $\sigma(F) = 0.41$ $F > 3.0$, $\sigma(F) = 0.41 + 0.0787\ (F - 3.0)$	$F < 0.6$, $\sigma(F) = 0.0$ $F \geq 0.6$, $\sigma(F) = 0.45 + 0.05\ (F - 0.6)$

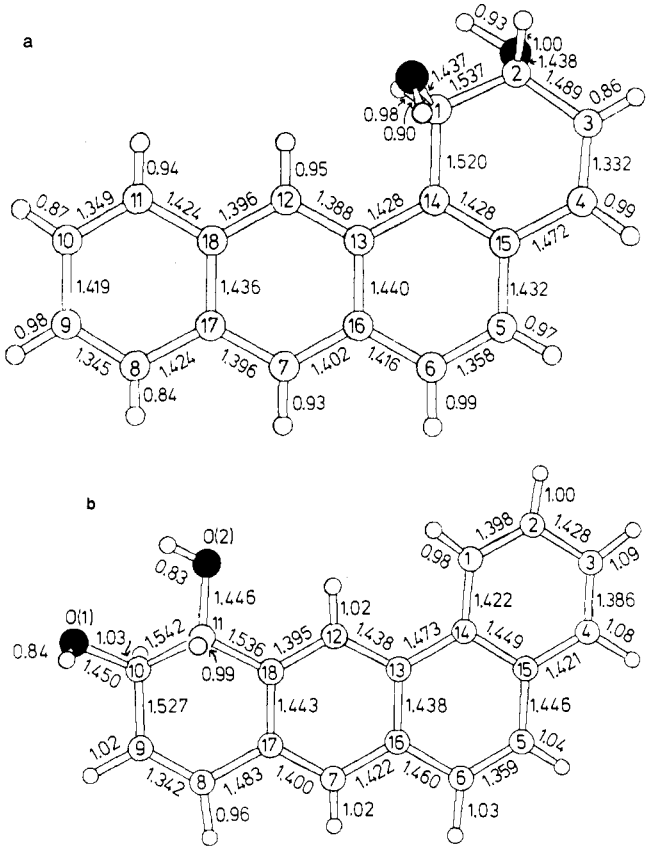

Figure 1. Interatomic distances in (a) molecule **1**, (b) molecule **2**. Estimated standard deviations, derived from the full-matrix least-squares calculation, are 0.002–0.003 Å for C–O distances, 0.002–0.004 Å for C–C distances, and 0.02–0.04 Å for C–H distances. Oxygen atoms are black.

responding diol epoxides and predict qualitatively the structures of other diol epoxides.

Since structural information on the dihydrodiols and their diol epoxide derivatives has, until now, been derived solely from NMR spectroscopic analysis, we were interested also in determining the correlation between information derived from the two techniques. As will be seen, X-ray and NMR analysis of the molecular configurations of compounds **1** and **2** are in substantial agreement.

Materials and Methods

(±)-*trans*-1,2-Dihydro-1,2-dihydroxybenz[*a*]anthracene (**1**) and (±)-*trans*-10,11-dihydro-10,11-dihydroxybenz[*a*]anthracene (**2**) were synthesized according to procedures described previously.[11,17-19] NMR spectra were taken on Varian T-60 and/or Bruker 270 MHz spectrometers in chloroform-*d*, acetone-d_6, or dimethyl-d_6 sulfoxide as indicated. Chemical shifts are relative to tetramethylsilane.

The crystal data for (±)-*trans*-1,2-dihydro-1,2-dihydroxybenz[*a*]anthracene (**1**) and (±)-*trans*-10,11-dihydro-10,11-dihydroxybenz[*a*]anthracene (**2**) are given in Table IA. Three-dimensional data were collected on a Syntex automated diffractometer (model $P2_1$ for **1**, model $P\bar{1}$ for **2**) with Cu Kα radiation (λ = 1.5418 Å) using the θ–2θ scan technique to $\sin\theta/\lambda$ = 0.61 Å^{-1}. Values for $\sigma(I)$ were derived from counting statistics and measured instrumental uncertainties (δ). Values for $\sigma(F)$ were calculated from the expression $(F/2)\cdot[\sigma^2(I)/I^2 + \delta^2]^{1/2}$. The intensity data were converted to structure amplitudes by application of Lorentz and polarization corrections and placed on an absolute scale with a Wilson plot. The monitoring of four standard reflections during the data collections showed no significant crystal decay. Further experimental details are in Table IB.

The structures were solved by direct methods using the MULTAN[20] series of programs. Refinement of the structures by Fourier and isotropic, then anisotropic, least-squares procedures gave residuals, R, for the observed data, of 0.105 for **1** and 0.099 for **2** for nonhydrogen atoms. Locations of the hydrogen atoms were determined from difference Fourier maps. Refinement was continued using isotropic temperature factors for the hydrogen atoms and anisotropic tem-

Table II. Final Atomic Parameters[a]

(±)-*trans*-1,2-Dihydro-1,2-dihydroxybenz[*a*]anthracene (**1**)

	x	*y*	*z*	b_{11}	b_{22}	b_{33}	b_{12}	b_{13}	b_{23}
O(1)	311 (1)	6457 (2)	1414 (1)	4.22 (4)	5.14 (6)	3.49 (5)	−0.52 (4)	1.15 (4)	−0.51 (4)
O(2)	639 (1)	6643 (2)	−1561 (1)	6.25 (6)	4.15 (5)	3.28 (5)	0.20 (4)	1.12 (5)	0.18 (4)
C(1)	939 (1)	6431 (2)	587 (2)	4.27 (6)	3.53 (6)	3.53 (6)	0.03 (5)	1.11 (6)	−0.08 (5)
C(2)	520 (1)	7487 (3)	−500 (2)	4.74 (6)	3.91 (7)	3.60 (7)	0.53 (6)	1.09 (9)	0.01 (3)
C(3)	920 (2)	9214 (3)	−520 (2)	6.78 (9)	3.69 (7)	4.44 (8)	0.98 (7)	1.37 (8)	0.60 (7)
C(4)	1753 (2)	9618 (3)	137 (2)	6.53 (9)	3.68 (7)	5.06 (9)	−0.39 (7)	1.91 (8)	0.14 (7)
C(5)	3266 (2)	8837 (3)	1474 (2)	5.03 (7)	4.46 (8)	6.72 (11)	−1.05 (7)	2.07 (8)	−0.29 (8)
C(6)	3809 (2)	7736 (3)	2208 (2)	4.40 (7)	5.34 (10)	6.66 (12)	−0.87 (7)	1.42 (8)	−0.75 (9)
C(7)	3988 (1)	5031 (3)	3260 (2)	3.73 (7)	6.02 (10)	5.55 (10)	0.14 (8)	0.54 (7)	−0.35 (9)
C(8)	4158 (2)	2340 (4)	4371 (2)	4.91 (8)	7.52 (13)	5.59 (11)	1.21 (10)	0.23 (8)	0.52 (10)
C(9)	3772 (2)	884 (4)	4641 (3)	6.34 (10)	7.55 (13)	5.88 (11)	2.13 (11)	1.35 (10)	2.23 (12)
C(10)	2841 (2)	418 (3)	4094 (2)	6.56 (10)	5.98 (11)	6.21 (11)	1.51 (9)	2.45 (10)	1.96 (10)
C(11)	2316 (2)	1462 (3)	3313 (2)	5.13 (8)	5.26 (9)	5.08 (10)	0.42 (7)	1.48 (8)	1.06 (8)
C(12)	2146 (1)	4159 (3)	2234 (2)	3.81 (6)	4.39 (7)	3.92 (7)	−0.15 (6)	0.78 (6)	0.22 (6)
C(13)	2489 (1)	5711 (3)	1956 (2)	4.13 (6)	4.16 (7)	3.68 (7)	0.02 (6)	1.17 (6)	−0.29 (6)
C(14)	1943 (1)	6886 (2)	1173 (2)	4.12 (6)	3.89 (7)	3.74 (7)	−0.04 (6)	1.38 (6)	−0.29 (6)
C(15)	2315 (2)	8407 (3)	945 (2)	5.15 (8)	3.76 (7)	4.60 (9)	−0.36 (6)	1.70 (7)	−0.34 (6)
C(16)	3441 (1)	6167 (3)	2488 (2)	3.89 (7)	4.83 (9)	4.95 (9)	−0.20 (6)	1.22 (7)	−0.55 (7)
C(17)	3631 (2)	3489 (3)	3556 (2)	4.32 (7)	5.63 (10)	4.57 (9)	0.85 (7)	0.82 (7)	0.08 (8)
C(18)	2684 (1)	3032 (3)	3011 (2)	4.36 (7)	4.93 (9)	4.02 (8)	0.52 (7)	1.24 (7)	0.22 (7)

	x	*y*	*z*	*B*		*x*	*y*	*z*	*B*
H(O1)	55 (2)	717 (3)	200 (2)	4.6 (5)	H(C6)	447 (2)	806 (4)	257 (3)	7.1 (7)
H(O2)	41 (2)	555 (5)	−153 (3)	6.9 (7)	H(C7)	461 (2)	529 (3)	359 (2)	4.7 (5)
H(C1)	90 (1)	529 (3)	27 (2)	3.9 (4)	H(C8)	465 (2)	276 (5)	478 (3)	7.9 (9)
H(C2)	−18 (2)	759 (4)	−58 (3)	6.1 (6)	H(C9)	419 (2)	12 (5)	516 (3)	7.9 (8)
H(C3)	58 (1)	993 (3)	−98 (2)	4.0 (4)	H(C10)	271 (2)	−63 (5)	419 (3)	7.1 (8)
H(C4)	198 (2)	1080 (4)	12 (3)	6.1 (6)	H(C11)	168 (2)	122 (4)	301 (3)	8.0 (8)
H(C5)	351 (2)	993 (4)	130 (2)	6.1 (6)	H(C12)	153 (2)	383 (3)	185 (2)	5.1 (5)

(±)-*trans*-10,11-Dihydro-10,11-dihydroxybenz[*a*]anthracene (**2**)

	x	*y*	*z*	b_{11}	b_{22}	b_{33}	b_{12}	b_{13}	b_{23}
O(1)	2182 (1)	6675 (1)	4913 (2)	4.65 (5)	5.62 (6)	5.50 (6)	0.81 (4)	0.24 (4)	1.22 (5)
O(2)	3570 (1)	7163 (1)	3586 (2)	4.62 (5)	3.85 (4)	5.54 (6)	0.46 (4)	0.55 (4)	−0.21 (4)
C(1)	6067 (1)	6598 (1)	1431 (3)	4.07 (7)	8.26 (12)	6.64 (11)	1.21 (8)	−0.67 (7)	−1.77 (10)
C(2)	6702 (1)	6790 (2)	610 (4)	4.65 (9)	11.08 (18)	8.42 (15)	0.79 (11)	0.11 (10)	−1.73 (14)
C(3)	7161 (1)	6248 (2)	−37 (4)	4.47 (9)	14.15 (22)	7.87 (15)	1.29 (12)	−0.22 (10)	−2.79 (17)
C(4)	6980 (1)	5543 (2)	169 (4)	5.03 (8)	12.46 (18)	6.11 (11)	3.19 (12)	−1.36 (8)	−3.31 (14)
C(5)	6149 (1)	4599 (1)	1191 (3)	7.46 (9)	8.88 (11)	4.83 (8)	4.54 (10)	−2.00 (8)	−2.44 (10)
C(6)	5523 (1)	4397 (1)	1922 (3)	8.25 (10)	6.35 (9)	4.89 (9)	3.37 (9)	−2.46 (9)	−1.76 (8)
C(7)	4344 (1)	4707 (1)	3218 (3)	7.19 (9)	4.50 (7)	4.38 (7)	1.35 (7)	−1.74 (7)	−0.64 (6)
C(8)	3122 (1)	4979 (1)	4368 (3)	7.16 (10)	4.60 (8)	4.67 (8)	−0.23 (7)	−0.92 (8)	0.33 (7)
C(9)	2586 (1)	5440 (1)	4509 (3)	5.73 (9)	5.17 (8)	5.18 (9)	−0.30 (7)	−0.55 (7)	0.59 (7)
C(10)	2683 (1)	6217 (1)	4012 (3)	4.56 (7)	4.96 (8)	4.07 (7)	0.26 (6)	−0.56 (6)	0.64 (6)
C(11)	3447 (1)	6471 (1)	4342 (2)	4.57 (7)	4.26 (7)	3.69 (6)	0.33 (5)	−0.39 (6)	−0.12 (5)
C(12)	4658 (1)	6161 (1)	3011 (3)	4.77 (7)	4.82 (7)	3.87 (7)	0.96 (6)	−0.91 (6)	−0.75 (6)
C(13)	5178 (1)	5662 (1)	2406 (2)	5.03 (7)	5.83 (8)	3.67 (7)	1.69 (6)	−1.45 (6)	−1.15 (6)
C(14)	5858 (1)	5880 (1)	1624 (3)	4.53 (7)	7.55 (11)	4.14 (7)	2.07 (7)	−1.39 (6)	−1.57 (7)
C(15)	6338 (1)	5336 (1)	1000 (3)	5.29 (8)	9.13 (13)	4.43 (8)	3.12 (9)	−1.72 (7)	−2.38 (9)
C(16)	5010 (1)	4921 (1)	2530 (3)	6.56 (9)	5.59 (9)	3.81 (7)	2.22 (8)	−1.94 (7)	−1.20 (7)
C(17)	3834 (1)	5200 (1)	3740 (3)	6.10 (9)	4.66 (8)	3.72 (7)	0.68 (7)	−1.35 (6)	−0.28 (6)
C(18)	3999 (1)	5944 (1)	3645 (2)	4.76 (7)	4.43 (7)	3.49 (6)	0.86 (6)	−0.95 (6)	−0.49 (5)

	x	*y*	*z*	*B*		*x*	*y*	*z*	*B*
H(O1)	218 (2)	657 (2)	599 (5)	8.4 (8)	H(C6)	538 (1)	387 (2)	205 (4)	6.6 (6)
H(O2)	326 (2)	743 (2)	396 (4)	8.1 (8)	H(C7)	422 (1)	418 (1)	328 (3)	5.8 (5)
H(C1)	575 (1)	697 (1)	186 (4)	7.3 (6)	H(C8)	309 (1)	448 (1)	458 (4)	6.9 (6)
H(C2)	686 (2)	729 (2)	47 (5)	10.6 (10)	H(C9)	209 (1)	531 (1)	487 (4)	6.5 (6)
H(C3)	764 (2)	643 (2)	−71 (5)	10.4 (9)	H(C10)	259 (1)	625 (1)	266 (3)	4.9 (5)
H(C4)	729 (2)	510 (2)	−31 (5)	9.3 (8)	H(C11)	352 (1)	651 (1)	564 (3)	4.7 (4)
H(C5)	651 (2)	421 (2)	84 (5)	9.1 (8)	H(C12)	478 (1)	669 (1)	297 (3)	5.0 (5)

[a] Positional parameters are given as fractions of cell edges $\times 10^4$ ($\times 10^3$ for hydrogen). Anisotropic temperature factors are expressed as $\exp[-\frac{1}{4}(h^2a^{*2}B_{11} + k^2b^{*2}B_{22} + l^2c^{*2}B_{33} + 2hka^*b^*B_{12} + 2hla^*c^*B_{13} + 2klb^*c^*B_{23})]$ and isotropic temperature factors as $\exp(-B\sin^2\theta/\lambda^2)$ with B values given in Å^2. The standard deviations for each parameter, determined from the inverted full matrix, are given in parentheses and applied to the last specified digits.

perature factors for the other atoms and with weights, w, of $1/\sigma^2(F)$ for data above the observation threshold and zero for the other data. The quantity minimized during the refinements was $\sum w||F_o| - |F_c||^2$.

Revised weights were derived from plots of $\langle||F_o| - |F_c||\rangle$ vs. $\langle F\rangle$ and were used in the final two refinement cycles. Weighting functions are given in Table IC, along with the final values for the residuals. The final atomic parameters are given in Table II.

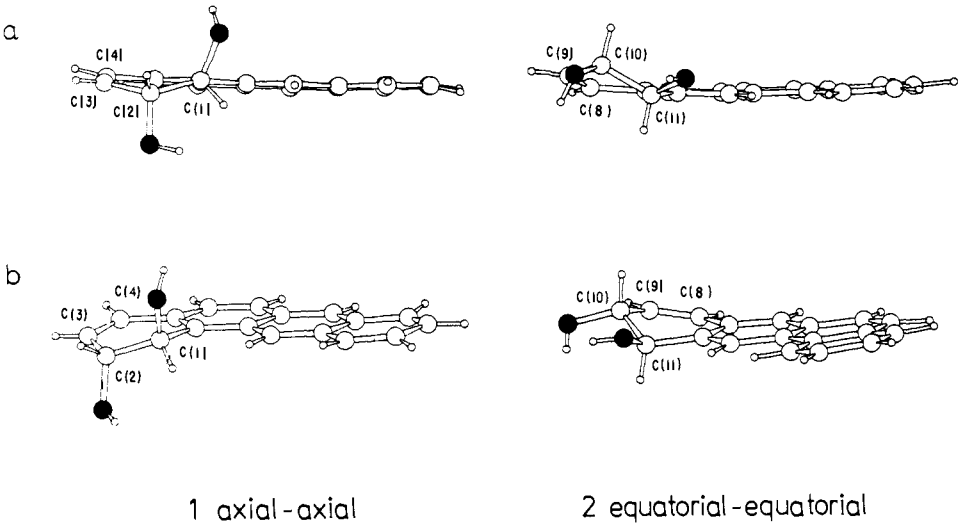

Figure 2. Views of the diols of **1** and **2**, showing the diaxial conformation of **1** and the diequatorial conformation of **2**. (a) View along the ring system. (b) General view. Oxygen atoms are black, carbon atoms are white, and hydrogen atoms are small.

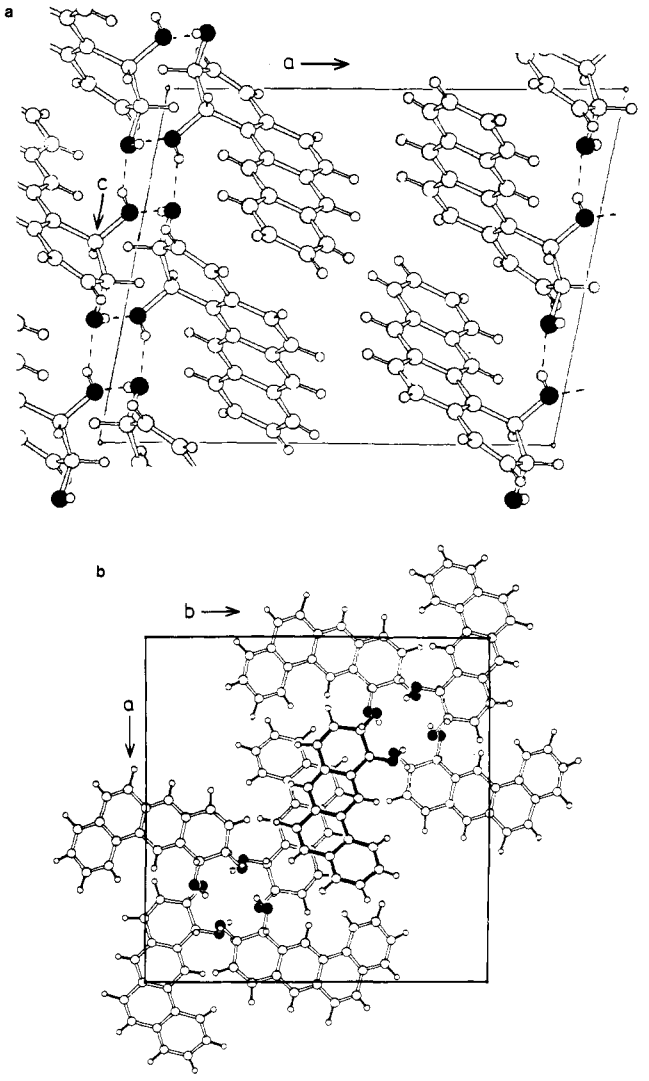

Figure 3. Packing of molecules in the unit cells of crystals. (a) View down b for molecule **1**. (b) View down e for molecule **2**. One molecule is marked in black for clarity. Atom designation as in Figure 2.

Atomic scattering factors for oxygen and carbon atoms were those given in the International Tables[21] and for hydrogen atoms those of Stewart, Davidson, and Simpson.[22] Computer programs used in these determinations were the CRYSNET[23] package, UCLALS4,[24] and other programs written in the Institute for Cancer Research Laboratory.

Table III. Angles between Planes in the Molecule (deg)

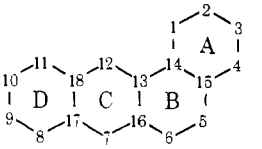

	1	2
A:B	8.01	2.28
A:C	7.42	5.23
A:D	6.63	17.25
B:C	0.94	2.95
B:D	2.87	15.01
C:D	2.50	12.03

Discussion of the Solid State Structure

Conformation of the Ring System. The unsubstituted ring system of each diol benz[*a*]anthracene is approximately planar as shown in Table IM (microfilm edition). All deviations, excluding those of the substituted rings (C(1) to C(4) for molecule **1**, C(8) to C(11) for molecule **2**), are less than 0.082 Å. Bond lengths are given in Figure 1 and interbond angles are listed in Table IIM (microfilm edition). The C–O bond lengths all lie in the range 1.437–1.450 Å (esd 0.002–0.003 Å). While the C–O bond lengths are slightly shorter in the axial (1.437, 1.438 Å) than equatorial (1.446, 1.450 Å) conformer, these differences may not be significant. The buckling of the substituted ring systems is illustrated in Figure 2 and some relevant torsion angles are listed in Table IIIM (microfilm edition). The two conformations, diaxial for **1** and diequatorial for **2**, are clearly shown in Figure 2. The substituted ring in **1** has a maximum torsion angle of −26.9° (14-1-2-3) while the least hindered substituted ring in **2** has a maximum torsion angle of 45.6° (18-11-10-9). In each case the surroundings of the double bond are nearly planar. The torsion angles involving O(1) and O(2) are −137.5° for **1** (O(1)-1-2-O(2)) and −64.1° for **2** (O(1)-10-11-O(2)), again illustrating the lesser distortion in **2** (anticipated values, based on an idealized carbon chain, would be 180 and −60°, respectively). The angles between planes of the various rings in the molecules are given in Table III. The maximum values are 8.01° in **1** and 17.25° in

Table IV. Hydrogen Bonding

D-H···A		D···A, Å	D···H, Å	H···A, Å	∠D-H···A, deg
		Molecule **1**			
O(1)-H(O1)···O(2)	$x, 1.5 - y, 0.5 + z$	2.753	0.90	1.90	158
O(2)-H(O2)···O(1)	$-x, 1 - y, -z$	2.837	0.93	1.92	167
		Molecule **2**			
O(1)-H(O1)···O(2)	$y - 0.5, 1 - x, 0.5 + z$	2.805	0.84	1.97	174
O(2)-H(O2)···O(1)	$0.5 - x, 1.5 - y, z$	2.801	0.83	2.02	158

Table V. Correlation between the Observed and Calculated Values of the Coupling Constants (J) of the Carbinol Hydrogen Atoms in the ^{1}H NMR Spectra of the 1,2- and 10,11-Dihydrodiols of Benz[*a*]anthracene[a]

isomer	dihedral angles, deg		calcd couplings, Hz		obsd couplings, Hz: diol, acetone-d_6	obsd couplings, Hz: diol, Me_2SO-d_6	obsd couplings, Hz: dibenzoate, $CDCl_3$
1	H_1-H_2	88 ± 6	$J_{1,2}$	2.0 ± 0.1	1.8	1.8	1.8
	H_2-H_3	36 ± 3	$J_{2,3}$	5.2 ± 0.2	5.0	5.0	5.6
2	H_{10}-H_{11}	172 ± 4	$J_{10,11}$	12.7 ± 0.2	10.0	9.5	6.3
	H_9-H_{10}	92 ± 5	$J_{9,10}$	2.6 ± 0.1	2.2	2.2	3.8

[a] Calculated coupling constants (J) were derived from the Karplus relationships as modified by Bothner-By[24] and Garbisch[25] employing the dihedral angles obtained from the X-ray data. The diols were exchanged with deuterium oxide prior to measurement of the spectra in order to simplify the spectra by elimination of couplings to the hydroxyl protons. The theoretically calculated values of $J_{1,2}$ and $J_{10,11}$ represent the couplings between the diequatorial protons of **1a,a** and the diaxial protons of **2e e** respectively.

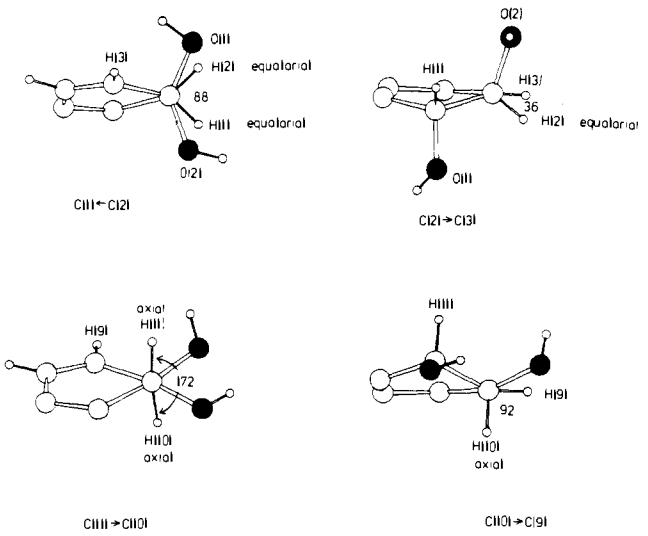

Figure 4. Views down C(2) → C(1) and C(2) → C(3) for molecule **1** and C(11) → C(10) and C(10) → C(9) for molecule **2**. This illustrates the torsion angles between certain hydrogen atoms that are measured in the X-ray experiment and used in the analysis of the NMR experiment (Table V).

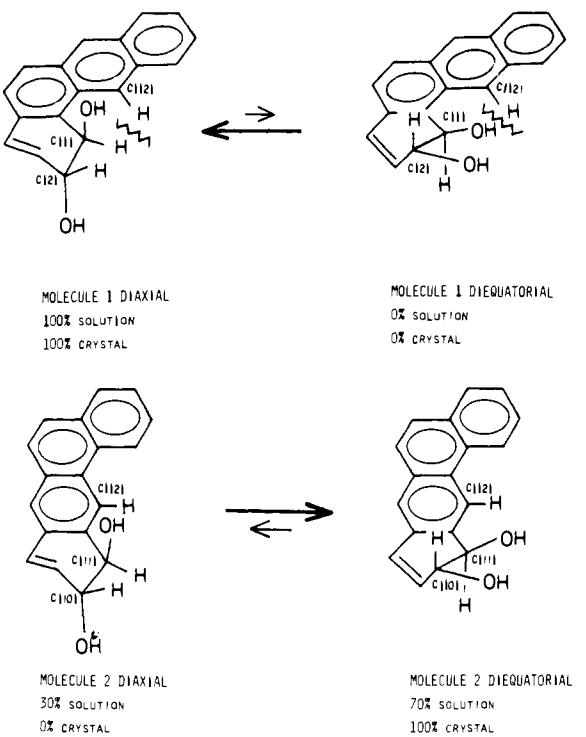

Figure 5. Diagrams of diaxial and diequatorial forms of the dihydrodiols of benz[*a*]anthracene indicating the population in the crystalline state and in solution.

2. The ring system is thus more planar in the more hindered molecule.

The packing of molecules in the unit cells is illustrated in Figures 3a (molecule **1**) and 3b (molecule **2**). Here the hydrogen bonding is evident and some relevant parameters are given in Table IV. There is no internal hydrogen bonding between the hydroxyl groups (as is also evident in Figure 1). Instead a network of hydrogen bonds extending through the crystal is formed. In Figure 3a the separation into hydrophilic and hydrophobic areas of the packing is illustrated.

NMR Spectral Analysis. Detailed analysis of the NMR spectra of the two dihydrodiols **1** and **2** provides results in remarkably good agreement with those derived from X-ray analysis. Coupling constants for the carbinol hydrogens (i.e., $J_{1,2}$ in **1** and $J_{10,11}$ in **2**) were calculated using the average torsion angles derived from the X-ray data (Figure 4) and the Karplus relationship (eq 1) as modified by Bothner-By.[25] Also couplings (i.e., $J_{2,3}$ in **1** and $J_{9,10}$ in **2**) were estimated using the Garbisch relation[26] (eq 2). Quite good agreement between the calculated and observed couplings was found, as shown in Table V.

$$^3J = 7 - \cos\phi + 5\cos 2\phi \quad (1)$$

$$^3J = \begin{cases} 4\cos^2\phi + 2.6 & (0° < \phi < 90°) \\ 9\cos^2\phi + 2.6 & (90° < \phi < 180°) \end{cases} \quad (2)$$

The calculated value of $J_{1,2}$ is 2.0 ± 0.1 Hz for the diaxial

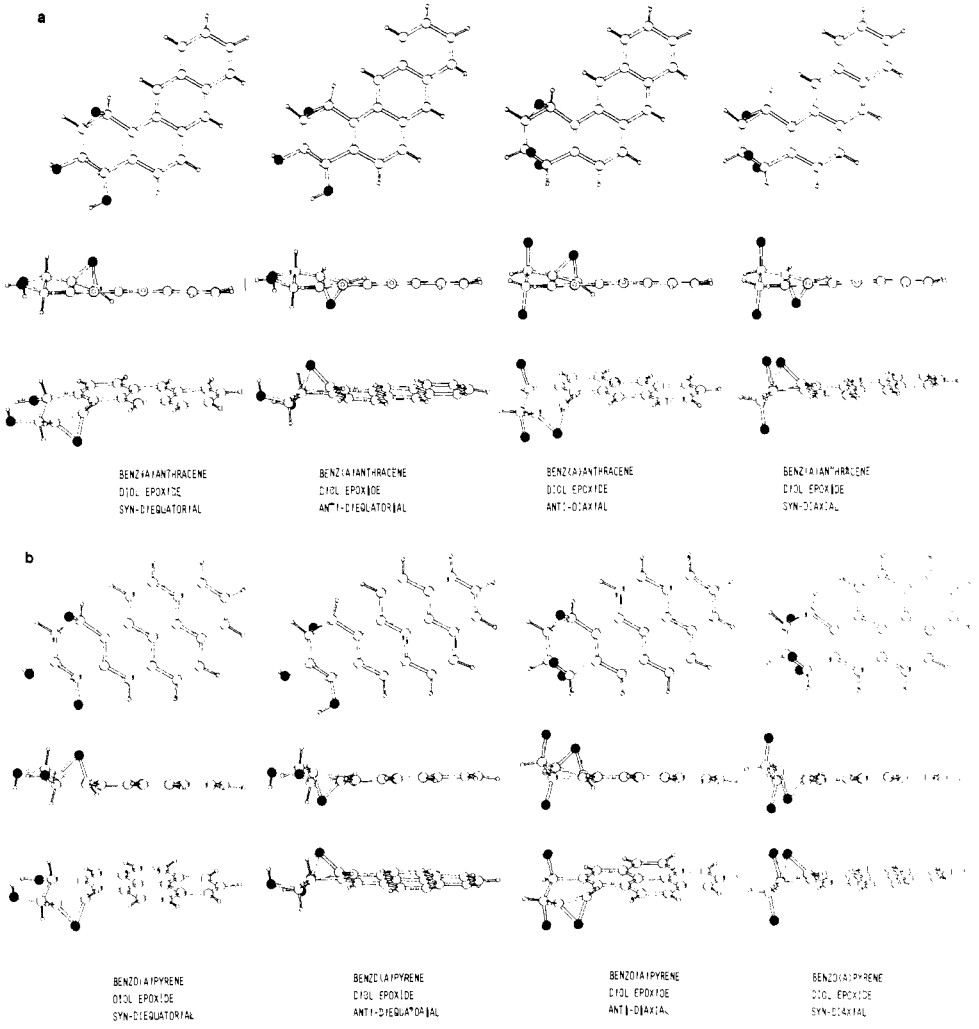

Figure 6. Views of dihydrodiol epoxides of benz[*a*]anthracene and benzo[*a*]pyrene computed from data on epoxides and dihydrodiols. Views are shown onto the plane of the cyclic ring system and onto the plane of the epoxide ring. (a) Benz[*a*]anthracene. (b) Benzo[*a*]pyrene. Coordinates are listed in Table IVM (microfilm edition).

Table VI. Coupling Constants of the Carbinol Hydrogens of the Bay Region Dihydrodiols and Diesters

dihydrodiol	obsd coupling, Hz	ref
3,4-phenanthrene	$J_{3,4} = 2$	27
diacetate	= 1.6	27
9,10-benzo[*a*]pyrene	$J_{9,10} \cong 2$	29
diacetate	=2	29
1,2-benz[*a*]anthracene	$J_{1,2} = 1.7$	27
diacetate	= 1.8	27
dibenzoate	$\cong 2$	29
3,4-chrysene	$J_{3,4} = 2$	31
dibenzoate	$J_{3,4} = 1.8$	30, 31
1,2-dibenz[*a*,*h*]anthracene	$J_{1,2} = 2$	29, 30
dibenzoate	$J_{1,2} = 2$	29
1,2-triphenylene	$J_{1,2} = 1$	32
dibenzoate	$J_{1,2} = 2$	32
9,10-benzo[*e*]pyrene	$J_{9,10} = 1.8$	32

conformer **1a,a,** and 1.8 Hz is observed experimentally. The calculated value of $J_{2,3}$ is 5.2 ± 0.2 Hz for **1a,a,** and 5.0 Hz is found experimentally. On the basis of these results, **1a,a** is deduced to be the sole conformation of the bay-region dihydrodiol both in solution as well as in the crystal lattice. It should be noted, however, that the values for the dihedral angles H_1–H_2 and H_2–H_3 (Figure 4) are also strained since the values are 88 and 36° in the diaxial conformer, instead of idealized values of 60 and 30°, respectively. This is presumably an effect due to the size of H(12).

Similar calculations performed on **2** predict the coupling constant $J_{10,11}$ = 12.7 ± 0.2 Hz for the diequatorial conformer. Experimentally determined values were 9.5 Hz in Me_2SO and 10.0 Hz in acetone. The calculated and observed values of $J_{9,10}$ were 2.6 ± 0.1 and 2.2 Hz, respectively. Since the observed couplings are less than anticipated for **2e,e** alone and considerably greater than expected for **2a,a**, this dihydrodiol must exist in solution as an equilibrium mixture of conformers undergoing interconversion rapidly on the NMR time scale.

Since the observed coupling can be presumed to be the weighted average of the ratio of conformers in solution, this ratio can be readily calculated. Assuming that the value of $J_{10,11}$ for **2a,a** equals $J_{1,2}$ = 2.0 Hz for **1a,a**, simple arithmetical calculation indicates the percentage of the diequatorial conformer **2e,e** in solution to be 70% in Me_2SO and 75% in acetone at ambient temperature. Alternatively, if the value of $J_{10,11}$ is derived not from **1a,a**, the geometry of which is slightly distorted as a consequence of the steric interaction between H(1) and H(12), but from an idealized dihedral angle for the carbinol hydrogens of 60°, then $J_{10,11} \cong 4.0$ Hz. With the latter value for the diaxial conformer **2a,a**, the percentages of **2e,e** in equilibrium with **2a,a** in solution in Me_2SO and acetone are calculated to be 60 and 70%, respectively. The lower ratio (i.e., approximately 70%) of **2e,e** in solution than in the crystal

(100%) is a consequence of several factors, one of which is the likely loss of intermolecular hydrogen bonding in the diequatorial form in chloroform solution.

The difference in preferred conformation of the two benz[*a*]anthracene dihydrodiols appears to be primarily a consequence of the steric interaction in the bay region of the 1,2-dihydrodiol. Conformational interconversion between **1a,a**, shown to be the sole form of **1** in solution, and **1e,e** is severely restricted as a consequence of steric interference between the relatively bulky hydroxyl group in the equatorial 1 position of the latter (Figure 5). A similar argument was advanced previously by Jerina et al.[27] to explain the diaxial conformational preference of the 1,2-dihydrodiol of phenanthrene deduced from NMR coupling constant data. It should be pointed out that conclusions concerning molecular structure based solely on NMR coupling constant data could be potentially misleading, since there are certain implicit assumptions (e.g., lack of serious molecular distortion and electronegativity effects on coupling) which could substantially alter the interpretation of such data. The present findings from X-ray crystallographic analysis of the structure of **1** provide the first direct experimental verification that the bay region dihydrodiol structure is not seriously distorted and the conclusions concerning conformation based on NMR analyses are valid.

Esterification of the 1,2-dihydrodiol had no discernible effect on $J_{1,2}$, showing that it is probably exclusively in the axial–axial conformation while $J_{10,11}$ of the 10,11-dihydrodiol decreased on dibenzoylation from 10.0 to 6.3 Hz (Table V). The ratio of conformers in solution is then calculated from the observed coupling to lie in the range of approximately 25–40% of **2e,e** (depending on which values are used to calculate coupling constants). Formation of the dibenzoate ester of **2** has two effects, both of which tend to shift the conformational equilibrium in favor of the diaxial structure. Intramolecular hydrogen bonding between the hydroxyl groups of **2e,e** which serves to stabilize this conformer in chloroform solution is lost and steric interaction between the bulky benzoate ester groups adjacent to one another favors formation of the diaxial conformer **2a,a** in which this effect is absent (Figure 2). However, these factors are insufficient to shift the equilibrium all the way to **2,a,a**, i.e., only to 60–75%. An alternative possibility which cannot be ruled out at present is that the diesters exist in a fixed conformation intermediate between the two extremes.

The NMR coupling constant data reported in the literature for other dihydrodiols and their diesters are also generally consistent with the present findings. In the case of the bay region dihydrodiols, the experimentally determined couplings of a relatively large series of free dihydrodiols and their diesters (Table VI)[27-32] exhibit relatively slight variation from the value of $J_{1,2}$ = 2.0 Hz observed for **1**, strong evidence that all these compounds also exist exclusively in the diaxial conformation. The only discrepancy is the value of $J_{1,2}$ = 3.8 Hz reported for the 1,2-dihydrodiol of dibenz[*a,h*]anthracene;[30] however, on reinvestigation we find $J_{1,2}$ = 2 Hz for both this compound and its dibenzoate diester. Thus, there is general agreement between the experimentally determined coupling constants and the value of $J_{e,e'}$ (2.0 ± 0.1 Hz) calculated from eq 1. Thus, the modified Karplus equation appears valid, at least empirically, for this system. Finally, it should be mentioned that Jeffrey et al.[28] calculated from Dreiding stereomodels a value of $J_{1,2}$ = 4.1 Hz for the coupling between the carbinol hydrogens of *trans*-1,2-dihydro-1,2-dihydroxynaphthalene in the diaxial conformation. The discrepancy from the value of $J_{1,2}$ = 2.0 Hz calculated herein results from the smaller dihedral angle (H_1–H_2 of 60°) assumed from the stereomodels vs. the experimental value (H_1–H_2 of 88°) obtained by X-ray analysis.

Diol Epoxides. Since detailed structural data from X-ray studies have now been obtained for cis and trans diols and for

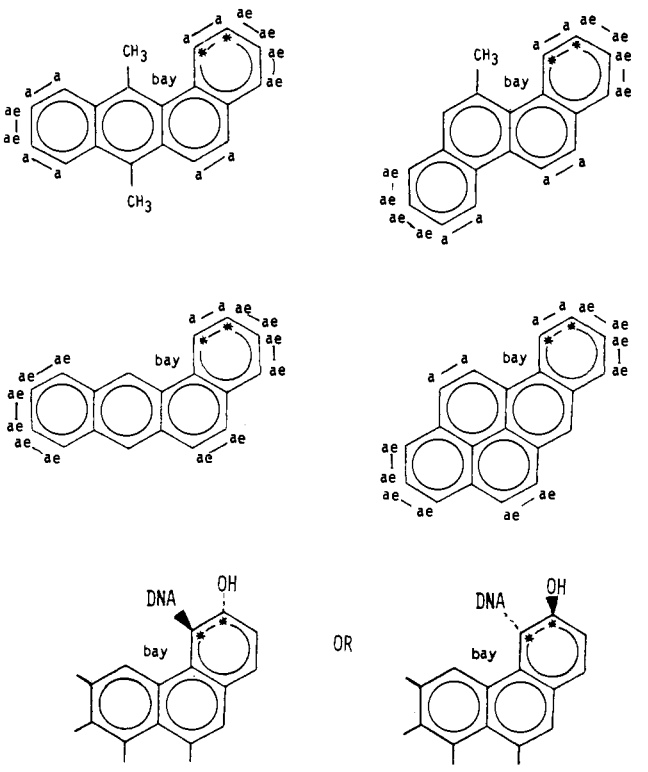

Figure 7. Conformations expected for the various diols of several carcinogenic polycyclic aromatic hydrocarbons. The bay region is marked. In each case the site of metabolic activation to an epoxide is indicated by an asterisk. In addition at each site the letter "a" means that a diol would be diaxial while "ae" indicates an equilibrium of axial and equatorial conformers. Diagrams are drawn for 7,12-dimethylbenz[*a*]anthracene, 5-methylchrysene, benz[*a*]anthracene, and benzo[*a*]pyrene. The axial attachment of a macromoleeule (possibly DNA) is shown at the bottom of the figure.

epoxides, the coordinates of the structures of the diol epoxides of benz[*a*]anthracene and benzo[*a*]pyrene, which are believed to be implicated in carcinogenesis, were calculated. The following stages were used in this calculation. The coordinates of benzo[*a*]pyrene[33] and its K-region[34] oxide have been determined by X-ray methods. These two structures contain a double bond and an epoxide group, respectively. The least-squares planes of the four carbon atoms that are part of or are adjacent to these groups were computed and a comparison of the results indicated the coordinate changes necessary to convert a double bond to an epoxide. These changes were then applied to the double bond (C(8)–C(9)) of the 10,11-dihydrodiol. In this way a ring containing a diol epoxide group was generated. Since there is very little buckling of the benzo[*a*]pyrene ring system on conversion from a hydrocarbon to an epoxide, it was assumed that the same would be true for the conversion of a dihydrodiol to a diol epoxide. The hydroxyl groups, which are diequatorial in this case, were converted to the diaxial conformation by interchanging hydrogen and hydroxyl groups. This was done because the positions of hydroxyl groups in the diol epoxides of interest are not hindered. Therefore, it was considered better to use the results from the nonhindered 10,11-dihydrodiol rather than the hindered (and strained) 1,2-diol. Finally the coordinates of the diol epoxide so generated were applied to benzo[*a*]pyrene[33] and to benz[*a*]anthracene (the 1,2-diol) by fitting the best plane through the two carbon atoms that would be fused to the diol epoxide ring and their two adjacent carbon atoms (C(13), C(14), C(15), and C(5) in the case of the 1,2-diol) to the least-squares plane through the analogous four atoms of the diol epoxide system (C(12), C(18), C(17), C(7) with appro-

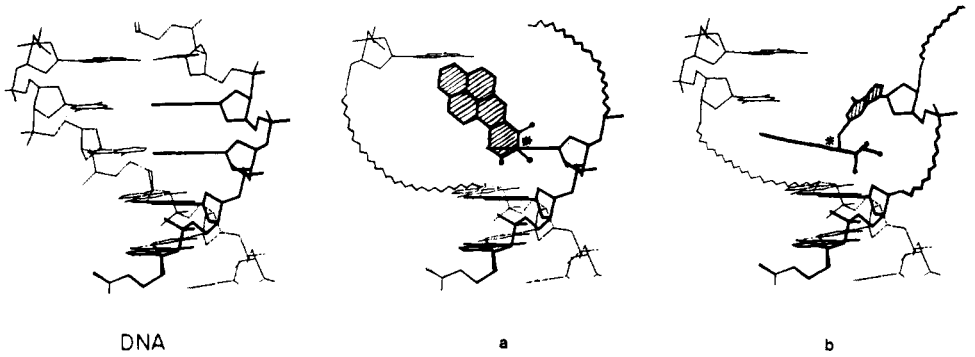

Figure 8. Diagram of possible modes of interaction of a dihydrodiol epoxide with a portion of a nucleic acid. In (a) the bulky hydrophobic group lies in a groove of DNA and in (b) it has swung in between the bases as suggested by Frenkel and co-workers.[46] In the diagram of the interaction with DNA the wavy line indicates an area of local denaturation (of unknown structure) caused by the presence of the bulky carcinogen.

priate inversion where necessary). The assumption in these calculations that the rings are not distorted by formation of a diol epoxide can only be tested when the crystal structure of a diol epoxide is determined. Unfortunately suitable crystals are not available to us at present. However, the coordinates listed in Tables IVMa and IVMb of the microfilm edition give an approximate view of the shapes of such molecules and the various O···O distances that might be expected. The results are illustrated in Figures 6a and 6b, respectively (with mirror image forms omitted), and coordinates are listed in Tables IVMa and IVMb (microfilm edition).

In general, the polycyclic arene portion of these molecules is essentially planar with the reactive epoxide ring at an angle of approximately 103° to the plane of the larger polycyclic ring system. Therefore, nucleophilic attack by an S_N2 mechanism would be anticipated to occur axially from the opposite face of the molecule at the reactive benzylic carbon atom of the epoxide ring. Indeed, it has been shown that the major product of binding of the *anti*-BP diol epoxide to DNA and RNA both in vivo and in vitro arises from trans addition of the 2-NH_2 group of guanosine to the C-10 position of the diol epoxide.[35-38] Molecular models indicate that the 2-NH_2 group of guanosine is relatively exposed in the minor groove of the DNA helix. Axial attack of the 2-NH_2-dG group on the epoxide ring requires orientation of BP diol epoxide within the minor groove approximately parallel to the long axis of the DNA helix. This suggests that a necessary structural requirement for carcinogenic activity is that molecular dimensions of the active metabolite not exceed the maximum permissible for insertion within the minor groove in this manner. The isomeric syn and anti diol epoxides of both BP and BA in Figures 6a and 6b fit this requirement. This structural limitation may partially account for the weak carcinogenic activity of molecules such as benzo[*e*]pyrene and larger polycyclic ring systems, insertion of the diol epoxides of which, in this manner, is less favorable.

The equatorial conformations of these diol epoxides are suggested to be favored over the diaxial forms by the NMR evidence[39,40] and by the X-ray analysis of the related dihydrodiols reported herein. Prior to the synthetic availability of the authentic anti and syn diol epoxides of BP,[39,40] it was suggested by Hulbert[41] that the syn isomer might be uniquely reactive as a consequence of transannular hydrogen bonding, and it was proposed that this isomer was the biologically active form. Chemical evidence in support of this idea was provided by Yagi et al.[39] Subsequent biological evidence, however, indicates that the anti isomer is the major form bound in vivo in mammalian cells.[35-38,42,43] The coordinates of the syn axial form of diol epoxides of BA and BP suggest that hydrogen bonding between the epoxide oxygen atom and the hydroxyl group on the β-carbon atom is possible since the two oxygen atoms approach within 2.7 Å of each other. In the anti axial form the epoxide oxygen atom and the hydroxyl oxygen atom on the α-carbon atom approach within 2.7 Å of each other, but the angular relationships are less suitable for an internal hydrogen bond. In aqueous solution, as in the crystalline state, one might not expect any internal hydrogen bonding. The extent to which oxygen–oxygen interactions stabilize one conformer over another is not known, although CNDO/2 calculations[9,44] indicate the stabilizing effect of internal hydrogen bonding in the syn axial conformer.

In each carcinogenic polycyclic aromatic hydrocarbon the steric effects on the conformations of dihydrodiols may be quickly established. Using the results obtained in this paper one can label each position as shown in Figure 7. In each case the site of metabolic activation to an epoxide ring in a diol epoxide is indicated by asterisks and in each case this is a position where the dihydrodiol would be diaxial because of some steric effect. In our X-ray crystallographic studies of the K-region cis dihydrodiol[16] of DMBA the 6-hydroxyl group is axial because of the presence of the nearby 7-methyl group. In the K-region oxide of DMBA[45] the arene oxide ring is asymmetric, the C(6)-O bond being longer than the C(5)-O bond. This suggests that one C-O bond of the epoxide, that is, the one nearer the 7-methyl group, is more readily broken, a deduction that is in line with chemical evidence. It is possible that similar factors are operative in the other systems shown in Figure 7 so that a carbonium ion is generated at the hindered site, and this is the site of attack of nucleic acid (illustrated diagrammatically in Figure 8) or nuclear protein.

Acknowledgment. This research was supported by Grants CA-10925, CA-06927, CA-22780, CA-11968, CA-14599, and RR-05539 from the National Institutes of Health, U.S. Public Health Service, BC-242 and BC-132 from the American Cancer Society, AG-370 from the National Science Foundation, and an appropriation from the Commonwealth of Pennsylvania.

Supplementary Material Available: Deviations from planarity in the phenanthrene-like portion of each molecule (Table IM), interbond angles (Table IIM), some torsion angles (Table IIIM), atomic coordinates (Table IVM), and coordinates, from group substitutions, of the diol epoxides of benzo[*a*]pyrene and benz[*a*]anthracene (calculated, not observed) (33 pages). Ordering information is given on any current masthead page. Tables of observed and calculated structure factors are available from the authors.

References and Notes

(1) (a) The Institute for Cancer Research, The Fox Chase Cancer Center; (b) The Ben May Laboratory for Cancer Research, The University of Chicago.
(2) P. Sims and P. L. Grover, *Adv. Cancer Res.*, **20**, 165 (1974).
(3) R. F. Newbold and P. Brookes, *Nature (London)*, **261**, 52 (1976).
(4) C. Malaveille, H. Bartsch, P. L. Grover, and P. Sims, *Biochem. Biophys. Res.*

Commun., **66**, 693 (1975).
(5) P. G. Wislocki, A. W. Wood, R. L. Chang, W. Levin, H. Yagi, O. Hernandez, D. M. Jerina, and A. H. Conney, *Biochem Biophys. Res. Commun.*, **68**, 1006 (1976).
(6) C. Malaveille, B. Tierney, P. L. Grover, P. Sims, and H. Bartsch, *Biochem. Biophys. Res. Commun.*, **75**, 427 (1977).
(7) A. N. Wood, R. L. Chang, W. Levin, R. E. Lehr, M. Schaefer-Ridder, J. M. Karle, D. M. Jerina, and A. H. Conney, *Proc. Natl. Acad. Sci. U.S.A.*, **74**, 2746 (1977).
(8) T. J. Slaga, E. Huberman, J. K. Selkirk, R. G. Harvey, and W. M. Bracken, *Cancer Res.*, **38**, 1699 (1978).
(9) D. R. Thakker, W. Levin, A. W. Wood, A. H. Conney, T. A. Stoming, and D. M. Jerina, *J. Am. Chem. Soc.*, **100**, 645 (1978).
(10) (a) A K region is defined as an aromatic bond, such as the 9,10 bond of phenanthrene, excision of which leaves an intact polycyclic ring system. (b) A bay region is a region of a polycyclic hydrocarbon between adjacent fused aromatic rings, such as the 4 and 5 positions of phenanthrene or the 1 and 12 positions of benz[*a*]anthracene.
(11) R. G. Harvey and P. P. Fu in "Polycyclic Hydrocarbons and Cancer: Environment, Chemistry and Metabolism", Vol. 1, H. V. Gelboin and P. O. P. Ts'o, Eds., Academic Press, New York, 1978, pp 133–163.
(12) H. W. S. King, M. R. Osborne, and P. Brookes, *Int. J. Cancer*, **20**, 564–571 (1977).
(13) R. C. Moschel, W. M. Baird, and A. Dipple, *Biochem. Biophys. Res. Commun.*, **76**, 1092 (1977).
(14) V. Ivanovic, N. E. Geacintov, A. M. Jeffrey, P. P. Fu, R. G. Harvey, and I. B. Weinstein, *Cancer Lett.*, **4**, 131 (1978); T. J. Slaga, G. L. Gleason, J. DiGiovanni, K. B. Sukumaran, and R. G. Harvey, *Cancer Res.*, **39**, 1934 (1979).
(15) W. Levin, D. R. Thakker, A. W. Wood, R. L. Chang, R. E. Lehr, D. M. Jerina, and A. H. Conney, *Cancer Res.*, **38**, 1705 (1978).
(16) D. E. Zacharias, J. P. Glusker, R. G. Harvey, and P. P. Fu, *Cancer Res.*, **37**, 775 (1977).
(17) R. G. Harvey and K. B. Sukumaran, *Tetrahedron Lett.*, 2387 (1977).
(18) P. P. Fu and R. G. Harvey, *Tetrahedron Lett.*, 2059 (1977).
(19) P. P. Fu, H. M. Lee, and R. G. Harvey, *Tetrahedron Lett.*, 551 (1978).
(20) G. Germain, P. Main, and M. M. Woolfson, *Acta Crystallogr., Sect. A*, **27**, 368 (1971).
(21) "International Tables for X-ray Crystallography", Vol. III, Kynoch Press, Birmingham, England, 1962, p 201.
(22) R. F. Stewart, E. R. Davidson, and W. T. Simpson, *J. Chem. Phys.*, **42**, 3175 (1965).
(23) H. J. Bernstein, L. C. Andrews, H. M. Berman, F. C. Bernstein, G. H. Campbell, H. L. Carrell, H. B. Chiang, W. C. Hamilton, D. D. Jones, D. Klunk, T. F. Koetzle, E. F. Meyer, C. N. Morimoto, S. S. Sevian, R. K. Stodola, M. M. Strongson, and T. V. Willoughby, "CRYSNET—a Network of Intelligent Remote Graphics Terminals," Second Annual AEC Scientific Computer Information Exchange Meetings, Proceedings of the Technical Program, 1974, pp 148–158. Brookhaven Report No. BNL-18803, Brookhaven National Laboratory, Upton, N.Y., 1974.
(24) P. K. Gantzel, R. A. Sparks, R. E. Long, and K. N. Trueblood, UCLALS4 Program in FORTRAN IV (modified by H. L. Carrell), 1969.
(25) A. A. Bothner-By, *Adv. Magn. Reson.*, **1**, 195 (1965).
(26) E. W. Garbisch, *J. Am. Chem. Soc.*, **88**, 5561 (1964).
(27) R. E. Lehr, M. Schaefer-Ridder, and D. M. Jerina, *J. Org. Chem.*, **42**, 736 (1977).
(28) A. M. Jeffrey, H. J. Yeh, D. M. Jerina, T. R. Patel, J. F. Davey, and D. T. Gibson, *Biochemistry*, **14**, 575 (1975).
(29) R. G. Harvey et al., in preparation.
(30) J. M. Karle, H. D. Mah, D. M. Jerina, and H. Yagi, *Tetrahedron Lett.*, 4021–4024 (1977).
(31) P. P. Fu and R. G. Harvey. *J. Org. Chem.*, submitted.
(32) R. G. Harvey, H. M. Lee, and N. Shyamasundar, *J. Org. Chem.*, **44**, 78 (1979).
(33) J. Iball, S. N. Scrimgeour, and D. W. Young, *Acta Crystallogr., Sect. B*, **32**, 328 (1976).
(34) J. P. Glusker, D. E. Zacharias, H. L. Carrell, P. P. Fu, and R. G. Harvey, *Cancer Res.*, **36**, 3951 (1976).
(35) A. M. Jeffrey, I. B. Weinstein, K. W. Jennette, K. Grzeskowiak, K. Nakanishi, R. G. Harvey, H. Autrup, and C. Harris, *Nature (London)*, **269**, 348 (1978).
(36) I. B. Weinstein, A. M. Jeffrey, K. W. Jennette, S. H. Blobstein, R. G. Harvey, C. Harris, H. Autrup, H. Kasai, and K. Nakanishi, *Science*, **193**, 592 (1976).
(37) A. M. Jeffrey, K. W. Jennette, S. H. Blobstein, I. B. Weinstein, F. A. Beland, R. G. Harvey, H. Kasai, I. Muira, and K. Nakanishi, *J. Am. Chem. Soc.*, **98**, 5714 (1976).
(38) K. Nakanishi, H. Kasai, H. Cho, R. G. Harvey, A. M. Jeffrey, K. W. Jennette, and I. B. Weinstein, *J. Am. Chem. Soc.*, **99**, 258 (1977).
(39) H. Yagi, O. Hernandez, and D. M. Jerina, *J. Am. Chem. Soc.*, **97**, 6881 (1975).
(40) F. A. Beland and R. G. Harvey, *J. Chem. Soc., Chem. Commun.*, 84 (1976).
(41) P. B. Hulbert, *Nature (London)*, **256**, 146 (1975).
(42) H. W. S. King, M. R. Osborne, F. A. Beland, R. G. Harvey, and P. Brookes, *Proc. Natl. Acad. Sci. U.S.A.*, **73**, 2679 (1976).
(43) M. Koreeda, P. D. Moore, P. G. Wislocki, W. Levin, A. H. Conney, H. Yagi, and D. M. Jerina, *Science*, **199**, 778 (1978).
(44) C. Y. Yeh, P. P. Fu, F. A. Beland, and R. G. Harvey, *Bioorg. Chem.*, **7**, 497 (1978).
(45) J. P. Glusker, H. L. Carrell, D. E. Zacharias, and R. G. Harvey, *Cancer Biochem. Biophys.*, **1**, 43 (1974).
(46) K. Frenkel, D. Younberger, M. Boublik, and I. B. Weinstein, *Biochemistry*, **17**, 1278 (1978).

Multinuclear NMR Study of Dibenzo-30-crown-10 Complexes with Sodium, Potassium, and Cesium Ions in Nonaqueous Solvents

Mojtaba Shamsipur and Alexander I. Popov*

Contribution from the Department of Chemistry, Michigan State University, East Lansing, Michigan 48824. *Received February 1, 1979*

Abstract: Nuclear magnetic resonances of ^{23}Na, ^{133}Cs, and ^{13}C nuclei were used to study the sodium, potassium, and cesium ion complexes with dibenzo-30-crown-10 (L) in nitromethane, acetonitrile, acetone, methanol, and pyridine solutions. Potassium and cesium ions formed 1:1 complexes, but in the case of the sodium ion three complexes with the respective stoichiometries Na_2L, Na_3L_2, and NaL were identified in solutions. The NMR data support the existence of a "wrap around" structure for Cs^+-DB30C10 complex in solution. The chemical shift of the ^{133}Cs resonance was studied as a function of DB30C10/Cs^+ mole ratio at various temperatures in different solvents and from these data $\Delta G°$, $\Delta H°$, and $\Delta S°$ values for the complexation reactions were calculated. In all cases the complexes were enthalpy stabilized but entropy destabilized.

Introduction

Since Pedersen's discovery of macrocyclic polyether (crown) compounds capable of forming stable complexes with the alkali ions[1] the studies of these ligands and of their complexes became a very popular field of research. A variety of physicochemical techniques have been used for such investigations,[2] the choice of a favorite technique being dictated by the systems studied as well as by the particular expertise of the investigators. In our case we found that the nuclear magnetic resonances of the alkali nuclei offer a very sensitive technique for the studies of changes in the immediate chemical environment of the alkali ions in solutions.[3]

It was of interest to us to study the interactions of alkali ions with a large crown ether capable of forming three-dimensional complexes with these ions. In fact it has been shown by Bush and Truter[4] that dibenzo-30-crown-10 (DB30C10) has a large

0002-7863/79/1501-4051$01.00/0